Hindawi
Journal of Sensors
Volume 2023, Article ID 9805959, 1 page
https://doi.org/10.1155/2023/9805959

*Retraction*

# Retracted: Polarization Characteristics of Electromagnetic Wave Sensing in Confined Space Based on Hybrid Algorithm

**Journal of Sensors**

Received 19 December 2023; Accepted 19 December 2023; Published 20 December 2023



This article has been retracted by Hindawi following an investigation undertaken by the publisher [1]. This investigation has uncovered evidence of one or more of the following indicators of systematic manipulation of the publication process:

(1) Discrepancies in scope
(2) Discrepancies in the description of the research reported
(3) Discrepancies between the availability of data and the research described
(4) Inappropriate citations
(5) Incoherent, meaningless and/or irrelevant content included in the article
(6) Manipulated or compromised peer review

The presence of these indicators undermines our confidence in the integrity of the article's content and we cannot, therefore, vouch for its reliability. Please note that this notice is intended solely to alert readers that the content of this article is unreliable. We have not investigated whether authors were aware of or involved in the systematic manipulation of the publication process.

Wiley and Hindawi regrets that the usual quality checks did not identify these issues before publication and have since put additional measures in place to safeguard research integrity.

We wish to credit our own Research Integrity and Research Publishing teams and anonymous and named external researchers and research integrity experts for contributing to this investigation.

The corresponding author, as the representative of all authors, has been given the opportunity to register their agreement or disagreement to this retraction. We have kept a record of any response received.

## References

[1] H. Zhang, "Polarization Characteristics of Electromagnetic Wave Sensing in Confined Space Based on Hybrid Algorithm," *Journal of Sensors*, vol. 2022, Article ID 1724428, 9 pages, 2022.

Hindawi
Journal of Sensors
Volume 2022, Article ID 1724428, 9 pages
https://doi.org/10.1155/2022/1724428

*Research Article*

# Polarization Characteristics of Electromagnetic Wave Sensing in Confined Space Based on Hybrid Algorithm

**Hao Zhang**

*Weinan Normal University, Weinan Shaanxi 714000, China*

Correspondence should be addressed to Hao Zhang; 14095104210013@hainanu.edu.cn

Received 3 March 2022; Revised 1 April 2022; Accepted 12 April 2022; Published 13 May 2022

Academic Editor: Pradeep Kumar Singh



In order to make better use of electromagnetic waves in communication, navigation, and radar, this invention offers a feature of software to study the polarization of electromagnetic waves in a limited space based on a hybrid algorithm. Using the double Gaussian model, the polarization software model was developed according to vector analysis, and the characteristics of the software at different angles of electromagnetic polarization under the plasma sheath, different peak electron densities, and different collision frequencies were studied in *S*-band. The results show that at peak electron densities of $10^{17}/m^3$ and collision frequencies of 0.01 GHz, 0.1 GHz, and 1 GHz, the reverse polarity angles are 53°, 76°, and 77°, respectively, and the higher the electron peak densities, the higher the ratio, and the more severe the degradation of the properties: at an angle of 60° to $10^{17}/m^3$, $10^{18}/m^3$, and $10^{19}/m^3$, the axial ratio of the electron peak density is -1.1.dB, -6.2 dB and -10.1 dB, respectively; the greater the frequency of the electromagnetic wave than the frequency of the collision, the more severe the axial degradation of the electromagnetic wave as the frequency of the electromagnetic wave approaches its frequency corresponding to the maximum electron density. Relationship characteristics were as follows: 2.8 GHz frequency equal to $10^{17}/m^3$ is the closest to 2.3 GHz electromagnetic frequency, and the axial ratio characteristics deteriorate and are more severe than other conditions; the heterologous medium designed in this paper has simple structure, thin thickness, and easy process preparation, which will have potential applications in radar stealth.



## 1. Introduction

Polarization state is a very important characteristic of electromagnetic wave, which can be used to identify, code, and sample the detection target, and the polarization transformation of electromagnetic wave can be widely used in high-tech fields such as communication, aerospace, and electronic warfare. Controlling the polarization state of electromagnetic waves through artificial methods has always been the goal that people want to achieve. Traditional methods to regulate electromagnetic waves include grating regulation, dichromatic crystal regulation, and regulation through birefringence effects: artificial isotropic media or metamaterials. In recent years, it has attracted wide attention from the academic community, which has special properties that many natural materials do not have, such as negative group velocity, negative refractive index, perfect imaging, inverse Doppler effect, and perfect absorption. It represents the characteristic of the orientation of the electric field intensity vector changing with time at a given point in space and is described by the track of the end point of the electric field intensity vector changing with time, and it is called linearly polarized if the trajectory is straight, circularly polarized if the trajectory is circular, and elliptically polarized if the trajectory is elliptical. The study of electromagnetic polarization has important applications in the fields of medium wave broadcast antenna, TV receiving antenna, antenna positioning on rocket, satellite communication antenna, electronic countermeasures, and so on.

When the electromagnetic wave with any polarization mode is incident at an oblique angle into the reentry plasma, the electromagnetic wave can be decomposed into parallel polarization component and vertical polarization component relative to the incident plane; however, since the reentry plasma has different transmission coefficients for parallel and vertical polarized waves, the transmitted electromagnetic wave passing through the plasma will have different polarization modes from the incident wave, and the polarization mode of the receiving antenna is set to be the same as that of the incident wave, which leads to the polarization mismatch between the receiving antenna and the received signal, and then causes the polarization mismatch loss in the communication link. However, the space vector characteristic of electromagnetic wave-polarization characteristic has not been studied systematically.

Therefore, it is necessary for the measurement and control communication signal with a fixed polarization mode, and it is necessary to study the polarization characteristics of the electromagnetic wave incident and reentering the plasma sheath. Plasma sheath is composed of free electrons, positively charged ions, and negatively charged ions, a large number of neutral particles are electrically neutral at macrolevel, and plasmas with certain spatial distribution characteristics exhibit remarkable collective behavior of unbound states. In the plasma sheath, the Coulomb force between charged particles is a long range force, and its effect is far greater than the collision effect caused by the local short-range force of charged particles; therefore, when a single charged particle is disturbed, the disturbance is transmitted to other charged particles through the Coulomb force interaction between charged particles, resulting in an obvious group effect. Especially, after electromagnetic wave incident into the plasma sheath, the movement of charged particles will be disturbed by external electromagnetic wave, and the charged particles inside the plasma sheath will have a significant collective resonance response process; furthermore, the electromagnetic field intensity fluctuation state is affected, which makes the electromagnetic wave and plasma have obvious coupling effect, and seriously affects the propagation characteristics of electromagnetic wave.

Based on this paper, we study the polarization software properties of the plasma sheath at different incidence angles, different peak electron densities, and different collision frequencies. The simulation software designed in this paper provides a three-dimensional animation effect of the theoretical knowledge of electromagnetic wave propagation, polarization, and transmission on the basis of previous research. Understand and master the relevant knowledge of electromagnetic waves.

The deterministic model is based on the theory of electromagnetic fields and electromagnetic waves, modeling the confined space environment and calculating and analyzing it through mathematical methods. In the modeling process, various environmental parameters need to be fully considered, and the calculation methods mainly include the solution of Maxwell's equations, physical optics methods, and mode analysis. The deterministic model can accurately model the confined space scene and obtain the radio wave propagation characteristics in the research scene, so as to analyze and integrate the radio wave propagation characteristics of different antennas, and obtain the characteristics of the radio wave coverage in the environment. At present, the widely used deterministic model methods in confined space include the following: ray tracing method, full wave analysis method, vector parabolic equation method, mode theory method, and hybrid calculation method.

Polarization describes the variation of the electric field vector along the propagation cross-section of electromagnetic wave with time. It reflects the vector property of electromagnetic wave. In addition to time domain, frequency domain, and spatial information, polarization is also an important information of electromagnetic wave [1]. Tereshchenko et al. studied the method of solving the inverse electromagnetic acoustic problem based on the measurement results of the low-frequency magnetic fields of two orthogonal antennas on the Kola Peninsula in the lithosphere with different electrical conductivities. The polarization characteristics of tangential magnetic field components are determined. The theoretical calculation is compared with the planar layered model of homogeneous layered wave propagation medium [2]. In order to study the influence of inhomogeneous media filled with scattered particles (e.g., precipitated particles) on the polarization characteristics of electromagnetic waves propagating in the media in a circular direction (e.g., right hand), Masalov et al. proposed a method to estimate the influence of wave polarization transformation on circular depolarization ratio. This method is based on the anisotropic polarization characteristics of the homogeneous region and the second region for the heterogeneous media and the azimuth representation of the polarization eigenbasis relative to the measurement basis [3]. Forte et al. proposed a new method to determine the polarization of electromagnetic waves using passive circuits. A passive circuit composed of cascaded Wilkinson power dividers is used to realize the mathematical operation required for recovering polarization. This technique is robust and simple and enables all necessary characteristic detection to determine incident wave polarization. It requires only two orthogonal linearly polarized antennas to measure the amplitude. Compared with classical methods, the accuracy and simplicity of this method are verified [4].

There are many research methods for electromagnetic wave characteristics. In order to combat active interference, Wang and University proposed an adaptive polarization filtering method based on dual-polarization radar [5]. Zhang et al. numerically simulated the propagation of electromagnetic waves in the inhomogeneous reentry plasma sheath by using the finite element analysis software COMSOL. By observing the distribution of electromagnetic field, the propagation characteristics of electromagnetic wave are analyzed. The *s*-polarized electromagnetic wave begins to decay as an exponential function at the cutoff position. When the real part of the dielectric constant of the plasma approaches 0, *p*-polarized waves undergo mode transformation, and the variation of reflection, transmission, and absorption coefficients with frequency is calculated and analyzed [6]. Based on the analysis of electromagnetic wave propagation theory and multimode theory, Zang et al. studied the influence of shape factor on electromagnetic wave propagation attenuation of rectangular roadway in high-order mode through computer simulation, and the simulation results show that when the shape factor of rectangular tunnel is constant, the attenuation of electromagnetic wave increases with the increase of electromagnetic wave transmission mode; in different modes, with the increase of the shape factor, the slope of the electromagnetic wave attenuation curve remains unchanged; in the horizontal polarization mode, with the increase of the shape factor, the attenuation of electromagnetic wave decreases first and then increases, and the attenuation rate is the lowest when the shape factor is 1.7. In the vertical polarization mode, the attenuation curve also tends to decrease first and then increase [7]. Gao et al. derived the electric field equation and magnetic field equation, analyzed the absorption boundary conditions and numerical stability conditions, and established a double-layer medium model to simulate the propagation characteristics of plane waves [8]. In order to understand the absorption mechanism of electromagnetic waves, Zuo et al. introduced the analysis and design of a miniaturized polarization-insensitive (metamaterial absorber, MMA) used to suppress electromagnetic interference in the microwave band: the MMA is composed of periodic double-open ring arrays printed on FR4 substrates with a thickness of 0.07$\lambda$0. CST simulation results show that the absorption rate of MMA is over 90% in the wide frequency range of 8.3 ~ 11.3GHz. The equivalent circuit model of MMA single cell was established to study its absorption characteristics and analyze the electric field and surface current distribution at absorption peak [9]. Chen et al. derived the Bhatnagar-Gross-Krook (BGK) collision model of inhomogeneous dusty plasma from the Boltzmann approximation equation. In the case of an external magnetic field, combined with the collision and charging effects of dusty plasma, the expression of the dielectric coefficient of dusty plasma in a completely ionized BGK collision is obtained. The reflection and transmission coefficients of electromagnetic waves under different external magnetic fields and dusty plasma parameters were calculated using the transfer matrix method, and the propagation characteristics of dusty plasma under the nonuniformly fully ionized BGK collision model were analyzed [10, 11]. Schreiber et al. studied the static picture simulation of the knowledge of the potential distribution of the coaxial line, the uniform plane electromagnetic wave propagation, the standing wave state, etc. [12].

The plasma electron density studied in this paper using double Gaussian model, according to the vector analysis of the polarization model, based on the theory of the electromagnetic wave propagation, polarization, transmission, can observe the form of electromagnetic waves from multiple angles, the *S* frequency band in different incidence angles, different peaks of polarization software density, and different collision frequencies. It is helpful to better understand and master the relevant knowledge of electromagnetic waves, so as to lay a good foundation for establishing a complete electromagnetic theory system.

## 2. Research Methods

*2.1. Characteristics of the Polarization Software for the Electromagnetic Waves.* The polarization of electromagnetic waves is usually defined by the way that the spatial orientation of the electric field vector at a fixed point in space varies with time. If the tip of the electric field vector is traced as a straight line in space with time, it is called linearly polarized wave. If the tip of the electric field vector traces a circle in space during propagation, it is called circularly polarized wave. If the trajectory traced by the tip of the electric field vector in space is an ellipse during propagation, it is an ellipse polarized wave.

Planar electromagnetic waves moving along the axis have no $E_z$ component and generally have $E_x$ and $E_y$ components, if the $E_y$ component is zero and there is only the $E_x$ component, we call that linear polarization in the $x$ direction. If we have an $E_y$ component but no $E_x$ component, we call this linear polarization in the $y$ direction.

In general, both $E_x$ and $E_y$ exist, and when receiving this electromagnetic wave, the electromagnetic wave containing horizontal and vertical components will be obtained. If the amplitude and phase of the electromagnetic wave of the two components are different, various electromagnetic waves with different polarization forms can be obtained.

Circularly polarized wave was as follows: if $\varphi_1$ differs from $\varphi_2$ by 90° or 270° phase angles, then

$$E_x = E_{xm} \cos\left(\omega t - kz + \varphi_1\right), \tag{1}$$

$$E_y = E_{ym} \cos\left(\omega t - kz + \varphi_2\right). \tag{2}$$

The synthesized electromagnetic field is

$$E = \sqrt{E_x^2 + E_y^2} = E_m = \text{constant}. \tag{3}$$

Its direction is

$$\text{tga} = \frac{E_y}{E_x} = tg(\omega t - kz + \varphi_1), \tag{4}$$

$$\alpha = \omega t - kz + \varphi_1, \tag{5}$$

which represents the resultant field amplitude that does not change with time, and its direction is a circularly polarized wave that rotates with time.

As shown in Figure 1, after the circularly polarized wave incident, the plasma sheath at the incident angle $\theta$, and after refraction and reflection in plasma sheath, it degenerates into elliptic polarized wave propagation process.

For the transmitted wave after the oblique incident of the circular polarized wave of right-handed (RHCP) in the reentry plasma, it can be written as

$$\vec{E}^{t}_{\text{RHCP}} = E^t_{\parallel}\vec{\nu}_{\parallel} + E^t_{\perp}\vec{\nu}_{\perp} = E_0\tilde{T}_{\parallel}\vec{\nu}_{\parallel} + jE_0\tilde{T}_{\perp}\vec{\nu}_{\perp}. \tag{6}$$

Then, the axial ratio formula of the transmitted wave after the oblique incident of right-handed circularly polarized wave and left-handed circularly polarized wave in the

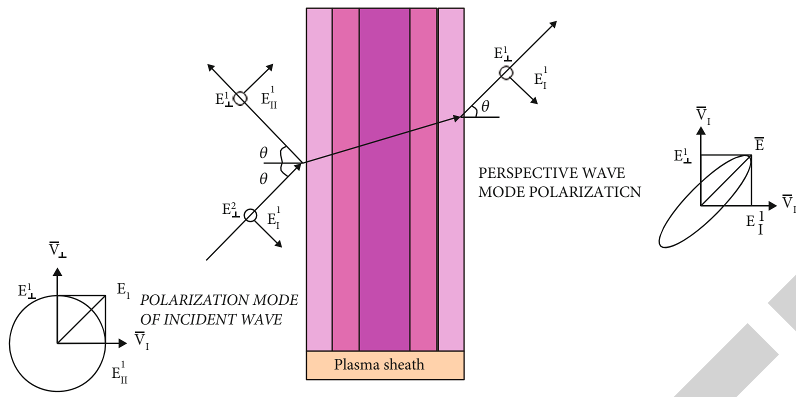


Figure 1: Schematic diagram of polarization mode change of circularly polarized electromagnetic wave at oblique incidence of plasma sheath.

reentry plasma can be expressed as

$$\mathrm{AR_{RHCP}} = \tan\left(\frac{1}{2}\arcsin\left(\frac{2\left|E_0\tilde{T}_{\parallel}\right|\left|jE_0\tilde{T}_{\perp}\right|\sin\phi^t_{\mathrm{RHCP}}}{\left|E_0\tilde{T}_{\parallel}\right|^2+\left|jE_0\tilde{T}_{\perp}\right|^2}\right)\right) = \tan\left(\frac{1}{2}\arcsin\left(\frac{2\left|\tilde{T}_{\parallel}\right|\left|\tilde{T}_{\perp}\right|\sin\phi^t_{\mathrm{RHCP}}}{\left|\tilde{T}_{\parallel}\right|^2+\left|\tilde{T}_{\perp}\right|^2}\right)\right). \quad (7)$$

Specifically, $\phi^t_{\mathrm{RHCP}}$ is calculated as follows:

$$\phi^t_{\mathrm{RHCP}} = \phi^t_{\perp} - \phi^t_{\parallel} = \arg\left(j\bullet E_0\bullet\tilde{T}_{\perp}\right) - \arg\left(E_0\bullet\tilde{T}_{\parallel}\right) = \arg\left(E_0\bullet\tilde{T}_{\perp}\right) - \arg\left(E_0\bullet\tilde{T}_{\parallel}\right) + 90^\circ. \quad (8)$$

*2.2. Electron Density Distribution of Plasma Sheath.* The electron density distribution of reentry plasma sheath is usually described by double exponential or double Gaussian models. The double Gaussian model is adopted, and its expression is

$$n_e(z) = n_{\mathrm{epeak}}\exp\left[-\alpha_1(z-z_0)^2\right] \quad 0 < z < z_0, \quad (9)$$

$$n_e(z) = n_{\mathrm{epeak}}\exp\left[-\alpha_2(z-z_0)^2\right] \quad 0 < z < z_t, \quad (10)$$

where $n_{\mathrm{epeak}}$ is the peak of electron density, $\alpha_1$ and $\alpha_2$ are the decay constants of the electron density in the sheath with distance, $z_0$ is the location of the maximum electron density, and $z_t$ is the thickness of plasma sheath. The flow chart of the hybrid algorithm model building for confined spatial wave propagation prediction is shown in Figure 2.

*2.3. Study on the Characteristics of Electromagnetic Wave Polarization Software*

*2.3.1. The Propagation of Electromagnetic Waves in the Unbounded Media.* Uniplane electromagnetic waves propagate in the ideal medium assuming the electric field only $x$ and the magnetic field only $y$. Then, the simplest physical

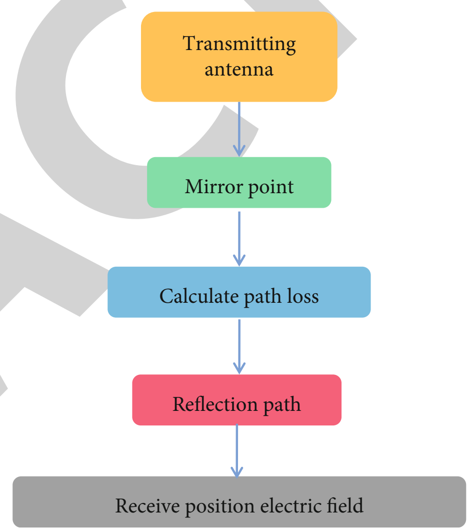


Figure 2: Flow chart of a hybrid algorithm model for confined spatial wave propagation prediction.

expression of the wave is shown in formulas (11) and (12):

$$\vec{E} = \vec{e}_x E_0 e^{-jkz}, \quad (11)$$

$$\vec{H} = \vec{e}_y \frac{E_0}{\eta} e^{-jkz}. \quad (12)$$

Equations (11) and (12) can summarize the characteristics of electromagnetic wave propagation in the ideal medium: first, the electric field and magnetic field amplitude proportional relationship, energy (amplitude), does not decay with time, second, no phase difference between the electric field and magnetic field, and finally, the electric field, right-handed, propagation direction. After simulation, a demonstration animation of electromagnetic wave propagation in an ideal medium is simulated.

In the simulation results of the electromagnetic wave polarization software that are in the first medium, the reflected wave amplitude is the opposite of the incident wave amplitude. The second medium has no wave. In the first medium, the incident wave and the reflected wave form a

Table 1: Changes in electron density and frequency.

| The sequence | Electron density (/m$^3$) | Frequency (GHz) |
|---|---|---|
| 1 | $10^{16}$ | 0.01 |
| 2 | $10^{17}$ | 0.1 |
| 3 | $10^{18}$ | 1 |
| 4 | $10^{19}$ | 10 |

resident wave. Resident waves are characterized by energy not propagating with the direction of propagation and only between the electric and magnetic fields.

To better illustrate that the reflected waves are linear polarized waves, the phase difference of the components of the reflected waves in the Pl and PZ directions was further analyzed. When the frequency is 12.0 9GHz, the phase difference between the Pl polarization component and the P2 polarization component is known from the electromagnetic wave theory that the reflected wave at 12.09 GHz, and the reflected wave is almost consistent with the P2 (PCR = 0.96 , PCR = PCR = 1); so, it fully proves that the linear polarization wave with the polarization direction is P2 after the designed artificial heterogeneous medium reflection is almost P2.The specific value of this deviation angle can be calculated in detail, because arctan (0.96/0.04) = 87.6; so, the specific deviation value is 2.4.

Based on the electromagnetic field and electromagnetic wave theory, antenna theory, and technology, the paper studies the radio wave coverage characteristics in confined space by using the numerical calculation method of hybrid electromagnetic field. The accuracy of the mixed method is verified by comparing the calculated results of the mixed method with the single numerical method and the measured data. The hybrid computing method proposed in this chapter provides an efficient tool for studying the radio coverage characteristics of multiple scenarios and complex confined spaces.

## 3. Results Analysis and Discussion

For the *S*-band measurement and control system, if the aircraft adopts the linear polarization transmission system, the movement of the aircraft will cause changes in the direction of electromagnetic wave polarization and causes polarization mismatch with the receiving system. However, if the aircraft adopts the circular polarization transmission system, it can not only resist the signal fluctuation caused by multipath but the double circular polarization classification technology can also improve the receiving system energy, and most ground stations use circular polarization receiving system. Therefore, this experiment takes the right-handed circularly polarized electromagnetic wave in *S*-band ($f = 2.3$ GHz) as an example, the polarization characteristics after passing through the plasma sheath at different angles and the loss of polarization mismatch between the transmitted wave and the receiving antenna were calculated, and the receiving antenna is a right-handed circularly polarized antenna. The plasma sheath is 10 cm thick, and the electron density is double Gaussian

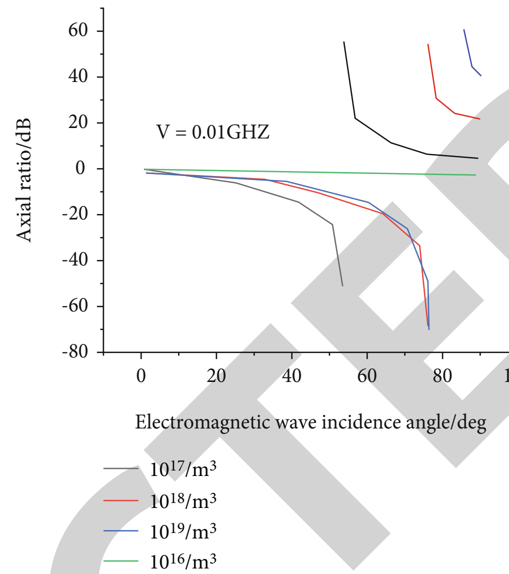


Figure 3: AR calculation results of transmitted wave axis ratio in *S* -band at $V = 0.01$ GHz.

distribution; among them, $\alpha 1 = 0.025$, $\alpha 2 = 0.025$, and z0 $= 0.05$ (see Table 1). The peak electron densities were $10^{16}$/m$^3$, $10^{17}$/m$^3$, $10^{18}$/m$^3$, and $10^{19}$/m$^3$, and the collision frequency was 0.01 GHz, 0.1 GHz, 1 GHz, and 10 GHz, respectively.

*3.1. Effect of Different Incidence Angles on the Characteristics of the Electromagnetic Wave Polarization Software.* In the case of different peak electron densities and different collision frequencies, the relation curve between the axial ratio AR and incident angle $\theta_0$ of the electromagnetic wave passing through the plasma sheath in the Beidou navigation frequency band was calculated, as shown in Figures 3–6. The collision frequency of Figure 3 is 0.01 GHz, that of Figure 4 is 0.1 GHz, that of Figure 5 is 1 GHz, and that of Figure 6 is 10 GHz.

The following conclusions can be drawn from the results in the figure:

(1) With the increase of incident angle, the characteristics of electromagnetic wave axis ratio are deteriorating. And the same as the navigation frequency band, when the incident angle is greater than a critical angle, the axial ratio of transmitted wave changes from negative to positive; in other words, the transmission wave changes from right-handed circular polarization wave to left-handed elliptic polarization wave, the polarization inversion phenomenon of electromagnetic wave occurs, and the electromagnetic wave depolarization effect is very serious

(2) When the incident angle of electromagnetic wave and the peak electron density of plasma sheath are constant, when the collision frequency is smaller, the worse the axial ratio of electromagnetic wave is, the smaller the critical angle of polarization reversal

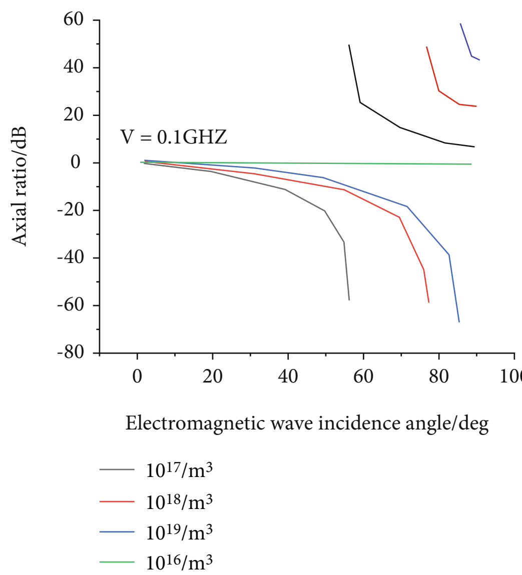


FIGURE 4: AR calculation results of *S*-band transmitted wave axial ratio when $V = 0.1$ GHz.

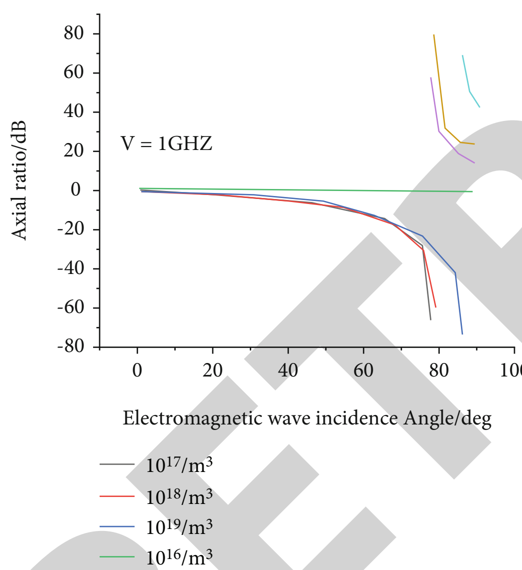


FIGURE 5: AR calculation results of transmitted wave axis ratio in *S* -band when $V = 1$ GHz.

is. As shown in Table 2, when the peak electron density is $10^{17}/m^3$ and the collision frequency is 0.01 GHz, 0.1 GHz, and 1 GHz, the critical angle of polarization reversal is 53°, 76°, and 77°, respectively

(3) When the electromagnetic frequency is less than the collision frequency, the deterioration degree of the electromagnetic wave axial ratio will increase with the increase of peak electron density. As shown in Table 3, the incident angle is 60°, and peak electron densities of $10^{17}/m^3$, $10^{18}/m^3$, and $10^{19}/m^3$ correspond to axial ratios of -1.1 dB, -6.2 dB, and

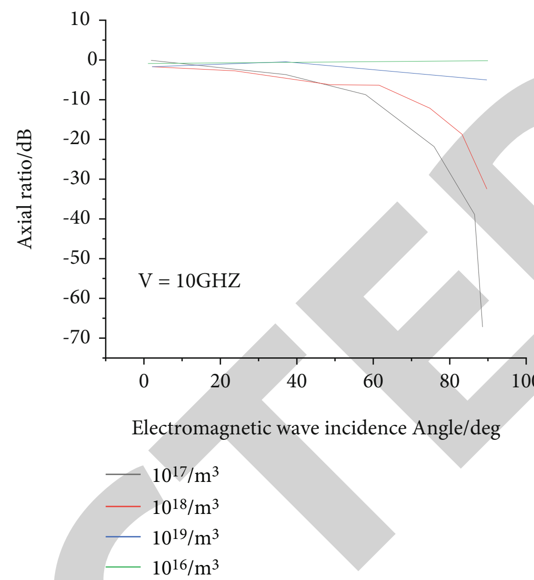


FIGURE 6: AR calculation results of transmitted wave axis ratio in *S* -band when $V = 10$ GHz.

-10.1 dB, respectively. When the electromagnetic frequency is greater than the collision frequency, the closer the electromagnetic frequency is to the characteristic frequency corresponding to the peak electron density, the worse the axial ratio of electromagnetic wave is. As shown in Table 4, the incident angle is 60°, and the collision frequency is 0.1 GHz, when the peak electron density is $10^{16}/m^3$, $10^{17}/m^3$, and $10^{18}/m^3$, the corresponding axial ratio is -0.5 dB, +22.2 dB, and -12.6 dB, respectively; among them, the characteristic frequency of $10^{17}/m^3$, 2.8 GHz, is the closest to the electromagnetic frequency, 2.3 GHz, and the deterioration of its axial ratio is more serious than other conditions

*3.2. The Effect of Incident Angle on the Phase Difference between Vertically Polarized and Parallel Polarized Waves.* In order to further study the polarization inversion phenomenon of *S*-band electromagnetic wave caused by plasma sheath, considering that the polarization direction of transmitted wave is related to the phase difference between vertical polarization and parallel polarization components, therefore, the phase difference of the two polarization components at different incident angles was calculated, as shown in Figures 7–10. The collision frequency of Figure 7 is 0.01 GHz, that of Figure 8 is 0.1 GHz, that of Figure 9 is 1 GHz, and that of Figure 10 is 10 GHz.

The following conclusions can be drawn from the results in the figure:

(1) When the plasma sheath parameter is constant, with the increase of the incidence angle of electromagnetic wave, the phase difference between vertical polarization and parallel polarization gradually changes from -90° to 90°, and when the incident

Table 2: Critical angle of polarization reversal for each collision frequency when peak electron density is $10^{17}/m^3$.

| Collision frequency (GHz) | Critical angle of polarization reversal (°) |
|---|---|
| 0.01 | 53 |
| 0.1 | 76 |
| 1 | 77 |

Table 3: Axial ratios of peak electron densities when the electromagnetic frequency is less than the collision frequency and the incident angle is 60°.

| Peak electron density ($/m^3$) | Axial ratio (dB) |
|---|---|
| $10^{17}$ | -1.1 |
| $10^{18}$ | -6.2 |
| $10^{19}$ | -10.1 |

Table 4: Axial ratios of peak electron densities when the electromagnetic frequency is greater than the collision frequency and the incident angle is 60°.

| Peak electron density ($/m^3$) | Axial ratio (dB) |
|---|---|
| $10^{16}$ | -0.5 |
| $10^{17}$ | -22.2 |
| $10^{18}$ | -12.6 |

angle is greater than a critical angle, the phase difference changes from negative value to positive value; at this time, the transmitted wave changes from right-handed circularly polarized wave to left-handed elliptically polarized wave, and the polarization inversion of the electromagnetic wave is consistent with the result given by the characteristic curve of the electromagnetic wave axial ratio [13]

(2) Comprehensive analysis of the curves shows that when the incidence angle of electromagnetic wave is larger, the collision frequency of plasma sheath is smaller, and the characteristic frequency corresponding to peak electron density is closer to the electromagnetic frequency; the larger the change of the phase difference between vertical polarization and parallel polarization components relative to -90°, the more serious the deterioration of the polarization characteristics of electromagnetic waves. Therefore, it can be concluded that the depolarization effect caused by the oblique incident electromagnetic wave is mainly caused by the change of the phase difference between the vertical polarization and the horizontal polarization components of the electromagnetic wave

## 4. Summary

This paper designs the characteristics of limited space electromagnetic wave polarization software based on a hybrid algorithm. The results show that at different frequency ranges, the isotropic medium can turn the incoming linear polarization wave into one perpendicular to its polarization, circular, and elliptic waves, which agrees with the results of numerical simulations. Further numerical analysis shows that the isotropic medium in the substrate nondestructive condition can transform the incoming ray polarized waves into linear and circular polarized waves perpendicular to them at different frequency bands, respectively. Therefore, the heterologous medium designed in this paper has simple structure, thin thickness, and easy process preparation, which will have potential applications in radar stealth.

The successful application of confined space electromagnetic field theory in many fields has promoted breakthrough

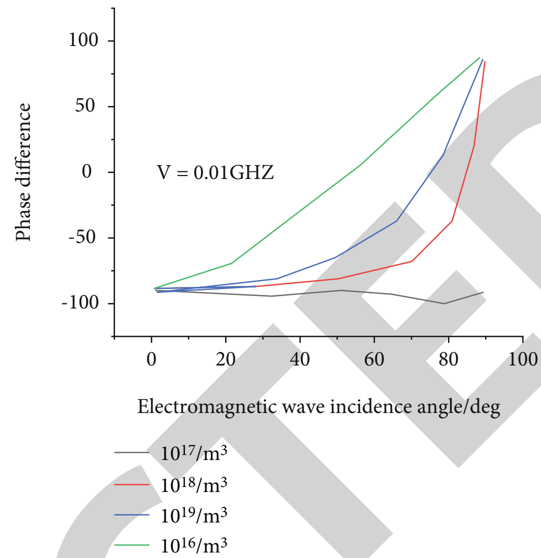


Figure 7: Phase difference between vertical and parallel polarized waves in $S$-band when $V = 0.01$ GHz.

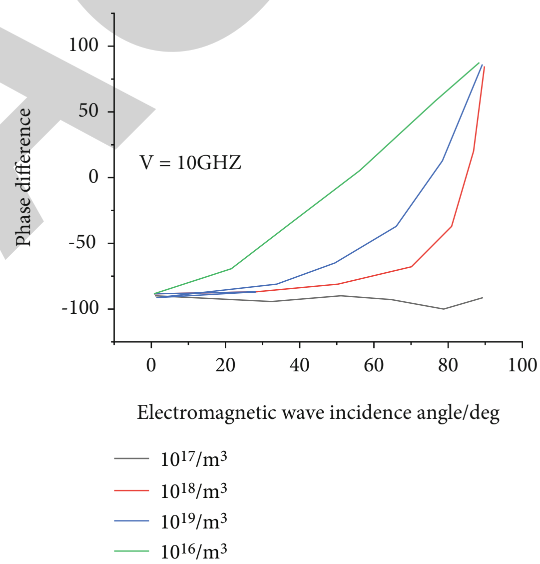


Figure 8: Phase difference between vertical and parallel polarized waves in $S$-band when $V = 0.1$ GHz.

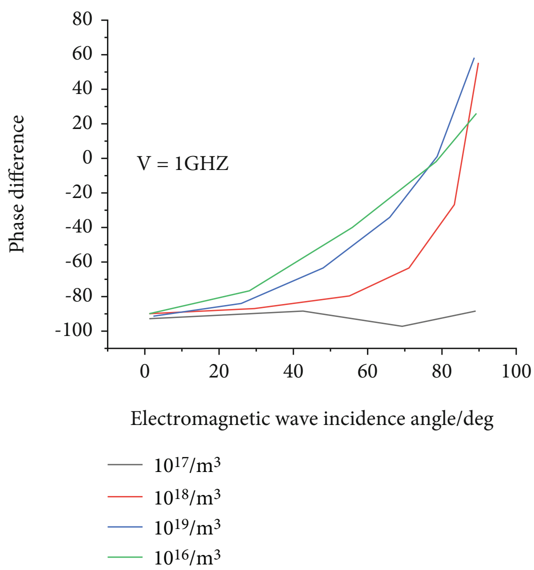


Figure 9: Phase difference between vertical and parallel polarized waves in *S*-band when $V = 1$ GHz.

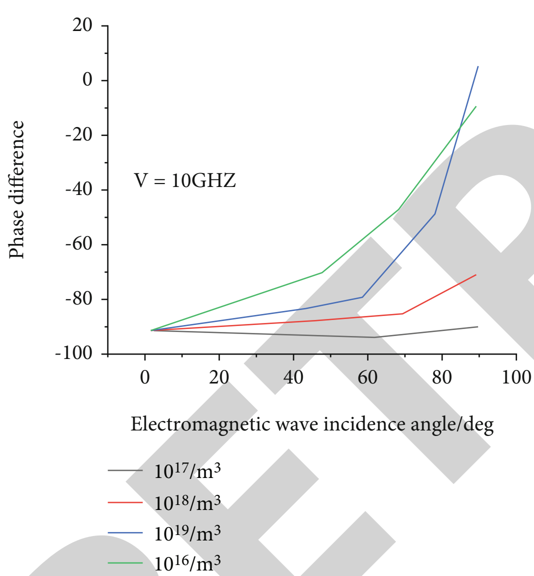


Figure 10: Phase difference between vertical and parallel polarized waves in *S*-band when $V = 10$ GHz.

development in various fields. In the future development of various fields, it is also inseparable from the research and application of electromagnetic fields. Among the many application fields of electromagnetic fields, the following brief description was as follows.

Several of these applications were as follows.

*4.1. New Electromagnetic Materials.* Science and technology is a powerful driving force for social progress and economic prosperity, and material science is an important cornerstone of the development of science and technology. The discovery and application of new materials are one of the fundamental driving forces for the development of science and technology. Artificial electromagnetic materials as new materials, with unique electromagnetic properties that natural materials do not have, have rapidly become an international research hot spot in recent years. The study of magnetic properties is indispensable in the field of artificial electromagnetic materials, and the development of electromagnetics is closely related to the research of new electromagnetic materials.

*4.2. Magnetic Levitation Technology.* Magnetic levitation technology is a technology that generates electromagnetic force by effectively combining multiple components such as sensors, controllers, electromagnets, and power amplifiers to levitate objects without mechanical contact. It is a very complex multidisciplinary integrated technology. In recent years, with scientists' research on electronic technology, control engineering, electromagnetic theory, and new electromagnetic materials, a breakthrough has been made in maglev technology, which has been widely used in aviation, railways, instruments, machinery manufacturing, and other fields, and electromagnetism is undoubtedly a crucial part of maglev technology.

## Data Availability

The data used to support the findings of this study are available from the corresponding author upon request.

## Conflicts of Interest

The author declares that he/she has no conflicts of interest.

## References


[1] H. Dai, X. Wang, X. Hong, S. Xiao, and L. Jia, *Connotation and Representation of Spatial Polarization Characteristic*, Springer, Singapore, 2019.

[2] E. D. Tereshchenko, P. E. Tereshchenko, and A. E. Sidorenko, "Polarization characteristics of the elf–slf magnetic field excited by a linear vibrator," *Seismic Instruments*, vol. 57, no. 3, pp. 321–328, 2021.

[3] E. V. Masalov, N. N. Krivin, and A. S. Rudometova, "Analysis of the variability of the circular depolarization ratio in remote sensing of an inhomogeneous medium," *Russian Physics Journal*, vol. 62, no. 1, pp. 147–155, 2019.

[4] G. Forte, G. Fontgalland, and H. S. Silva, "Polarization detection of electromagnetic waves using cascaded wilkinson power dividers," *IEEE Microwave and Wireless Components Letters*, vol. 30, no. 8, pp. 833–835, 2020.

[5] X. Wang, "Influence of shape factor of rectangular roadway on electromagnetic waves under high-order mode," *Industry and Mine Automation*, vol. 45, no. 5, pp. 68–72, 2019.

[6] Q. Zhang, R. Zhou, X. Shi, and Y. Zhao, "Adaptive dual-polarization filtering method for countering active jamming," *International Journal of Antennas and Propagation*, vol. 2020, no. 4, Article ID 4961402, p. 7, 2020.

[7] J. Zhang, Y. Liu, X. Li, L. Shi, and B. Bai, "2d simulation of the electromagnetic wave across the non-uniform reentry plasma sheath with comsol," *AIP Advances*, vol. 9, no. 5, article 055316, 2019.

[8] L. Gao, M. Li, F. Liu, and L. Zhang, "Numerical simulation of the plane electromagnetic wave transient propagation in lossy

medium," *IOP Conference Series: Materials Science and Engineering*, vol. 799, no. 1, article 012014, 2020.

[9] P. Zuo, T. Li, M. Wang, H. Zheng, and E. P. Li, "Miniaturized polarization insensitive metamaterial absorber applied on emi suppression," *IEEE Access*, vol. 8, pp. 6583–6590, 2020.

[10] W. Chen, Z. Wang, L. Yang, Z. Huang, and L. Wang, "Research on electromagnetic wave propagation characteristics of fully ionized inhomogeneous dusty plasma in a magnetized bgk model," *IEEE Transactions on Plasma Science*, vol. 49, no. 4, pp. 1460–1467, 2021.

[11] K. Xie, B. Sun, S. Guo, L. Quan, and Y. Liu, "Experimental apparatus for investigating the propagation characteristics of the low-frequency electromagnetic waves in hypersonic plasma fluid generated by shock tube," *Review of Scientific Instruments*, vol. 90, no. 7, article 073503, 2019.

[12] J. Schreiber, A. Balbaa, and C. L. Bottasso, "Brief communication: a double-gaussian wake model," *Wind Energy Science*, vol. 5, no. 1, pp. 237–244, 2020.

[13] G. Dhiman, K. K. Singh, M. Soni, A. Nagar, and K. Cengiz, "Mosoa: a new multi-objective seagull optimization algorithm," *Expert Systems with Applications*, vol. 167, article 114150, 2020.